



# The geometry of the statistical model for range-based localization

Marco Compagnoni

Algebraic Statistics 2015

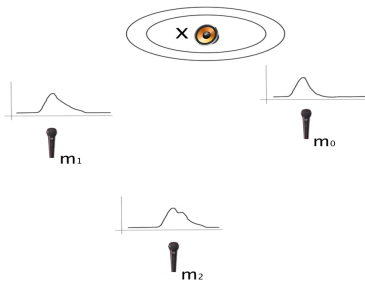
Genova, Italy

June 9, 2015

Joint work with Roberto Notari, Andrea Ruggiu, Fabio Antonacci and Augusto Sarti.

# Range-based Localization

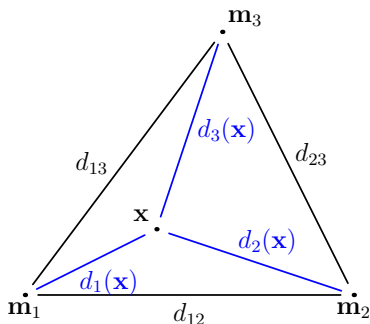
**Problem:** find the position of a point  $\mathbf{x}$  from the range measurements between  $\mathbf{x}$  and a set of given points  $\mathbf{m}_i$ ,  $i = 1, \dots, n$ .



## Examples of applications:

- radar and active sonar
- molecular conformation
- wireless sensor networks

## The Range Model



$$\mathbf{d}_i(\mathbf{x}) = \mathbf{x} - \mathbf{m}_i \quad d_i(\mathbf{x}) = \|\mathbf{d}_i(\mathbf{x})\|$$

$$\mathbf{d}_{ji} = \mathbf{m}_j - \mathbf{m}_i \quad d_{ji} = \|\mathbf{d}_{ji}\|$$

$$\mathcal{T}_{r,n} : \mathbb{R}^r \longrightarrow \mathbb{R}^n$$

$$\mathbf{x} \longmapsto (d_1(\mathbf{x}), \dots, d_n(\mathbf{x}))$$

$$\hat{d}_i(\mathbf{x}) = \text{measured range} \Rightarrow$$

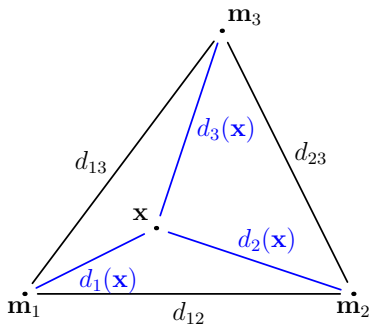
$$\epsilon_i = \text{measurement error}$$

$$\hat{d}_i(\mathbf{x}) = d_i(\mathbf{x}) + \epsilon_i$$

**The model:**  $\hat{\mathcal{T}}_{r,n}(\mathbf{x}) = (\hat{d}_1(\mathbf{x}), \dots, \hat{d}_n(\mathbf{x})) \sim N(\mathcal{T}(\mathbf{x}), \Sigma)$

- **Deterministic problem:** if  $\epsilon_i = 0$ , find the conditions for existence and uniqueness of  $\mathbf{x}$  (the identifiability problem).
- **Statistical problem:** if  $\epsilon_i \neq 0$ , efficiently estimate  $\mathbf{x}$ .

## Euclidean Distance Geometry



The deterministic problem is a main topic of **Euclidean Distance Geometry** (DG) [Liberti and others, 2014].

Given a weighted graph  $G = (V, E, W)$ , with

- $V$  the points  $m_i$  and  $x$
- $E$  the available distances
- $W$  the measured ranges

is  $G$  embeddable into some  $k$ -dimensional Euclidean space?

In DG the answer is usually given in terms of **Cayley–Menger determinant**.

## The set of feasible ranges

### Hypothesis:

- a point  $\mathbf{x} \in \mathbb{R}^2$ , thus  $r = 2$ ;
- three known points  $\mathbf{m}_1, \mathbf{m}_2, \mathbf{m}_3 \in \mathbb{R}^2$ , thus  $n = 3$ .

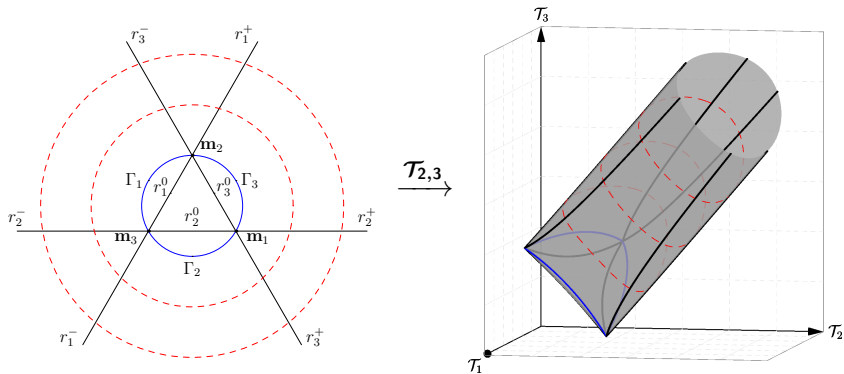
$\mathcal{T} = (\mathcal{T}_1, \mathcal{T}_2, \mathcal{T}_3) \in \text{Im}(\mathcal{T}_{2,3})$  if and only if

$$\begin{vmatrix} 0 & 1 & 1 & 1 & 1 \\ 1 & 0 & d_{12}^2 & d_{13}^2 & \mathcal{T}_1^2 \\ 1 & d_{12}^2 & 0 & d_{23}^2 & \mathcal{T}_2^2 \\ 1 & d_{13}^2 & d_{23}^2 & 0 & \mathcal{T}_3^2 \\ 1 & \mathcal{T}_1^2 & \mathcal{T}_2^2 & \mathcal{T}_3^2 & 0 \end{vmatrix} = 0, \quad \mathcal{T}_1, \mathcal{T}_2, \mathcal{T}_3 \geq 0.$$

**Proposition:** the set of feasible ranges is the semialgebraic surface  $X \subset \mathbb{R}^3$  defined by

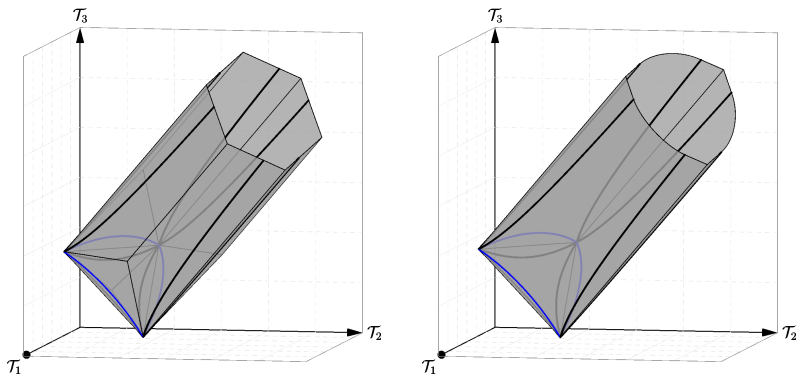
$$\begin{cases} d_{32}^2 \mathcal{T}_1^4 + d_{31}^2 \mathcal{T}_2^4 + d_{21}^2 \mathcal{T}_3^4 - 2\mathbf{d}_{32} \cdot \mathbf{d}_{31} \mathcal{T}_1^2 \mathcal{T}_2^2 + 2\mathbf{d}_{32} \cdot \mathbf{d}_{21} \mathcal{T}_1^2 \mathcal{T}_3^2 - 2\mathbf{d}_{31} \cdot \mathbf{d}_{21} \mathcal{T}_2^2 \mathcal{T}_3^2 - \\ - 2\mathbf{d}_{21} \cdot \mathbf{d}_{31} d_{32}^2 \mathcal{T}_1^2 + 2\mathbf{d}_{32} \cdot \mathbf{d}_{21} d_{31}^2 \mathcal{T}_2^2 - 2\mathbf{d}_{32} \cdot \mathbf{d}_{31} d_{21}^2 \mathcal{T}_3^2 + d_{21}^2 d_{31}^2 d_{32}^2 = 0, \\ \mathcal{T}_1, \mathcal{T}_2, \mathcal{T}_3 \geq 0. \end{cases}$$

## The Kummer's surface I



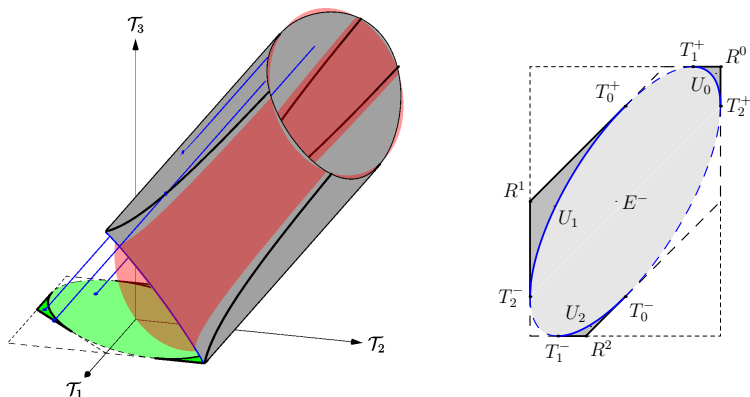
- $\bar{X}$  is a quartic surface with 16 nodes, thus  $\bar{X}$  is a **Kummer's surface**. The nodes on  $X$  are the images of  $\mathbf{m}_1, \mathbf{m}_2, \mathbf{m}_3$ .
- There exist 16 conics on  $\bar{X}$ . The conics on  $X$  are the images of  $r_i^\pm$  and  $\Gamma_i$ ,  $i = 1, 2, 3$ . They are asymptotic curves of  $X$  and divide the positive and negative curvature regions of  $X$ .

## The Kummer's surface II



- There exist 16 planes (the tropes), each one tangent to  $\bar{X}$  along one conic. The 12 tropes tangent to  $X$  come from the triangular inequalities plus some other geometrical arguments and they define a convex polyhedron  $Q_3$  containing  $X$ .
- The boundary of the convex hull of  $X$  is the union of the positive curvature regions of  $X$  and slices of each facet of  $Q_3$ .

## Pseudorange-based localization



- In some applications only the range differences or **pseudoranges** are available:  $\tau_1(\mathbf{x}) = d_1(\mathbf{x}) - d_3(\mathbf{x})$ ,  $\tau_2(\mathbf{x}) = d_2(\mathbf{x}) - d_3(\mathbf{x})$  [Compagnoni and others, 2013].
- The set of feasible pseudoranges is the projection  $\pi(X)$  of  $X$  from its ideal singular point, where  $\pi(\mathcal{T}_1, \mathcal{T}_2, \mathcal{T}_3) = (\mathcal{T}_1 - \mathcal{T}_3, \mathcal{T}_2 - \mathcal{T}_3)$ .

## Near and Far Field

In several applications one distinguishes between near and far field scenarios (e.g. distributed sensors versus compact arrays).

- **Near Field:** the point  $\mathbf{x}$  is closed to (at least one)  $\mathbf{m}_i$ ,  $i = 1, 2, 3$ . The **range model is singular**.
- **Far Field:** the point  $\mathbf{x}$  is far away from  $\mathbf{m}_i$ ,  $i = 1, 2, 3$ . A good approximation of the Kummer's surface is given by **the tangent cone to the ideal singular point of  $X$** , i.e. the elliptic cylinder  $C$  having equation

$$d_{32}^2 \mathcal{T}_1^2 + d_{31}^2 \mathcal{T}_2^2 + d_{21}^2 \mathcal{T}_3^2 - 2\mathbf{d}_{31} \cdot \mathbf{d}_{32} \mathcal{T}_1 \mathcal{T}_2 + 2\mathbf{d}_{21} \cdot \mathbf{d}_{32} \mathcal{T}_1 \mathcal{T}_3 - 2\mathbf{d}_{21} \cdot \mathbf{d}_{31} \mathcal{T}_2 \mathcal{T}_3 - \|\mathbf{d}_{31} \wedge \mathbf{d}_{32}\|^2 = 0.$$

## Far Field estimation

### Maximum Likelihood Estimation (MLE):

$$\bar{\mathcal{T}} = \underset{\mathcal{T} \in X}{\operatorname{argmin}} \|\hat{\mathcal{T}} - \mathcal{T}\|^2$$

- asymptotically efficient estimator;
- nonconvex optimization;
- $X$  has Euclidean Distance degree 20.

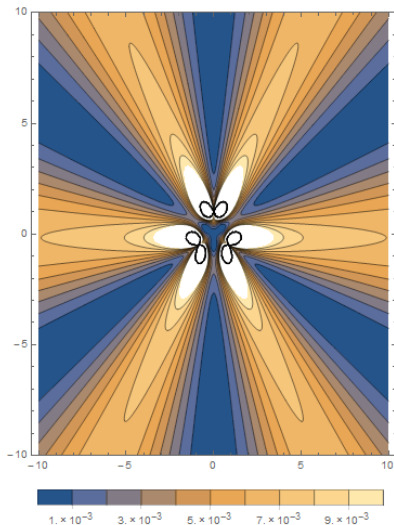
### Squared-Range-based Least Square (SR-LS):

[Beck,Stoica,Li 2008]

$$\bar{\mathcal{T}} = \underset{\mathcal{T} \in X}{\operatorname{argmin}} \|\hat{\mathcal{T}}^2 - \mathcal{T}^2\|^2$$

- it is not first order efficient;
- although nonconvex, there exist efficient solution methods;
- it is equivalent to MLE with respect to Cayley-Menger variety, an elliptic paraboloid with Euclidean Distance degree 5.

## SR-LS performance



### Scenario:

$$\mathbf{m}_1 = \left(-\frac{\sqrt{3}}{2}, -\frac{1}{2}\right), \quad \mathbf{m}_2 = \left(\frac{\sqrt{3}}{2}, -\frac{1}{2}\right), \quad \mathbf{m}_3 = (0, 1)$$

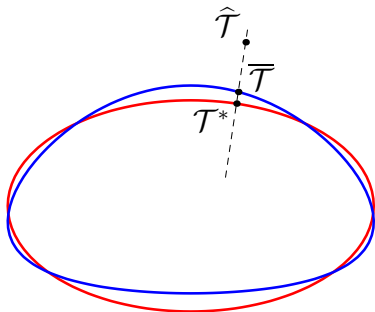
$$\hat{\mathcal{T}}(\mathbf{x}) \sim N(\mathcal{T}(\mathbf{x}), \sigma^2 \mathbf{I}), \quad \sigma = 0.1$$

### Asymptotic Inference:

- the inverse  $G(\mathbf{x})$  of the Fisher matrix gives the asymptotic mean square error of the MLE;
- by Cramér-Rao inequality, the asymptotic mean square error  $\bar{G}(\mathbf{x})$  of any consistent and unbiased estimator satisfies  $\bar{G}(\mathbf{x}) - G(\mathbf{x}) \succeq 0$ .

**Proposition:**  $\bar{G}(\mathbf{x}) - G(\mathbf{x})$  has only a non-zero eigenvalue  $\lambda(\mathbf{x})$ .

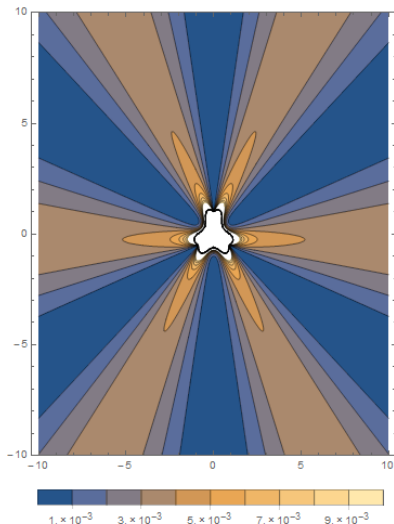
## Orthogonal projection on $C$



### Algorithm (OPC):

- find the nearest point  $\mathcal{T}^* \in C$  to  $\hat{\mathcal{T}}$ ;
- find the line  $L_{\hat{\mathcal{T}}}$  containing  $\hat{\mathcal{T}}, \mathcal{T}^*$ ;
- the estimate  $\bar{\mathcal{T}}$  is the intersection of  $L_{\hat{\mathcal{T}}}$  and  $X$  closest to  $\hat{\mathcal{T}}$ .

- OPC is a **consistent estimator**;
- the orthogonal projection on  $C$  is a two dimensional problem with Euclidean Distance degree 4, then to find  $L_{\hat{\mathcal{T}}} \cap X$  we have to solve a degree 4 polynomial equation;
- in far field regime we expect to have existence and uniqueness of the solution of OPC (at least in a local setting).



## OPC performance

### Scenario:

$$\mathbf{m}_1 = \left(-\frac{\sqrt{3}}{2}, -\frac{1}{2}\right), \quad \mathbf{m}_2 = \left(\frac{\sqrt{3}}{2}, -\frac{1}{2}\right), \quad \mathbf{m}_3 = (0, 1)$$

$$\hat{\mathcal{T}}(\mathbf{x}) \sim N(\mathcal{T}(\mathbf{x}), \sigma^2 \mathbf{I}), \quad \sigma = 0.1$$

### Results:

- **OPC performs better than SR-LS in far field regime**, while it is not suitable for near field localization;
- OPC has a **lower algebraic computational complexity** with respect to MLE;
- similar results have been obtained for more general sensor configurations and in the analysis of the bias.

# Conclusions and Perspectives

## In our work:

- we studied the range-based localization problem with two and three sensors in terms of real algebraic geometry;
- we have characterized the measurements space using classical results on Kummer's surfaces;
- we began the study of the estimation problem.

## In future works we will:

- complete the analysis of near and far field estimation (singular model, second order efficient estimators [Kobayashi,Wynn 2013]);
- extend our analysis to the cases with  $n > 3$  sensors.

## Bibliography



M.Compagnoni, R. Notari, A.A. Ruggiu, F.Antonacci, A.Sarti, *The Algebro-Geometric Study of Range Maps*, preprint, 2015.



L. Liberti, C. Lavor, N. Maculan, and A. Mucherino. *Euclidean distance geometry and applications*, SIAM REVIEW, 56(1):3-69, 2014.



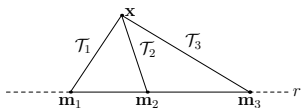
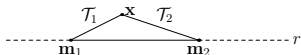
R.W.H.T. Hudson. *Kummer's quartic surface*, Cambridge University Press, 1990.



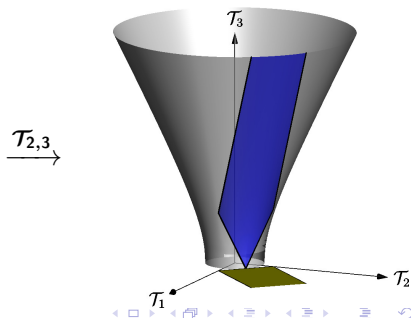
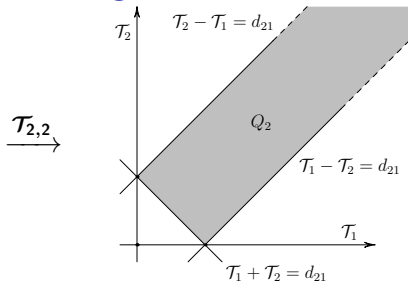
M.Compagnoni, R. Notari, F.Antonacci, A.Sarti, *A comprehensive analysis of the geometry of tdoa maps in localization problems*, Inverse Problems, 30(3):035004, 2014.



A. Beck, P. Stoica, and Jian Li. *Exact and approximate solutions of source localization problems*, IEEE Transactions on Signal Processing (TSP), 56:1770-1778, 2008.



## Aligned sensors



## SR-LS versus OPC

